

## Supplementary materials

### *Open water*

We visually examined the spatial pattern of 0m/s estimates from the NSIDC's Polar Pathfinder data set. These patterns roughly correspond to the known pattern of ice formation and melt, and therefore feel confident in our decision to remove these estimates under the assumption that they represent open water (Fig S1). The unusual pattern in July is likely an artefact in the data, caused by the quantization of ice motion estimates (Lavergne et al. 2010). This quantization error can result in large areas with the same vector, and this can appear as wavy or irregular patterns. It is not generally regarded as a large issue, nor was it present in the mean drift speeds over the entire HB (Fig. 3).

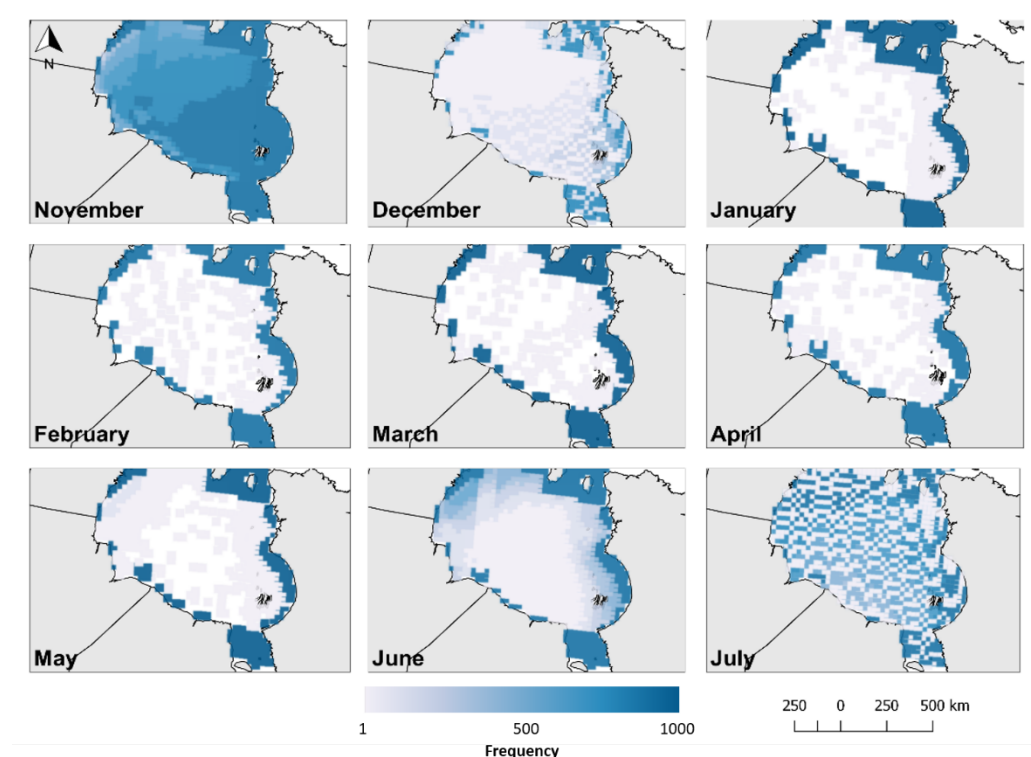


Fig S1. Spatial frequency of 0m/s estimates in Polar Pathfinder 25km EASE-Grid Sea Ice Motion Vectors from 1987-2015 in November-July.

### Gridded ice drift arefication

After calculating Moran's  $I$  on 100 days of ice drift data, we determined that grid points should be  $< 150$  km apart (Moran's  $I > 0.6$ ) to reduce spatial autocorrelation. To rarefy to this resolution (i.e., to ensure no grid points are closer than 150 km), we used a random sampling scheme to eliminate points within 150 km of each other. First, we randomly selected any grid point from the entire set. We then eliminated any grid point within 150 km of the randomly selected grid point. We then randomly selected another grid point from the remaining points and repeated the process. This was repeated on the data set until no grid points were within 150 km of one another. We want the maximum amount of grid points that still satisfy the criteria of being 150 km apart, but there is nothing in this process to maximize the new data set. Therefore, we repeated the process 10,000 times (i.e., produced 10,000 rarefied data sets) and selected the data set with the most remaining grid points (27 unique grid points with 166,755 rows of ice drift data; Fig. S2).

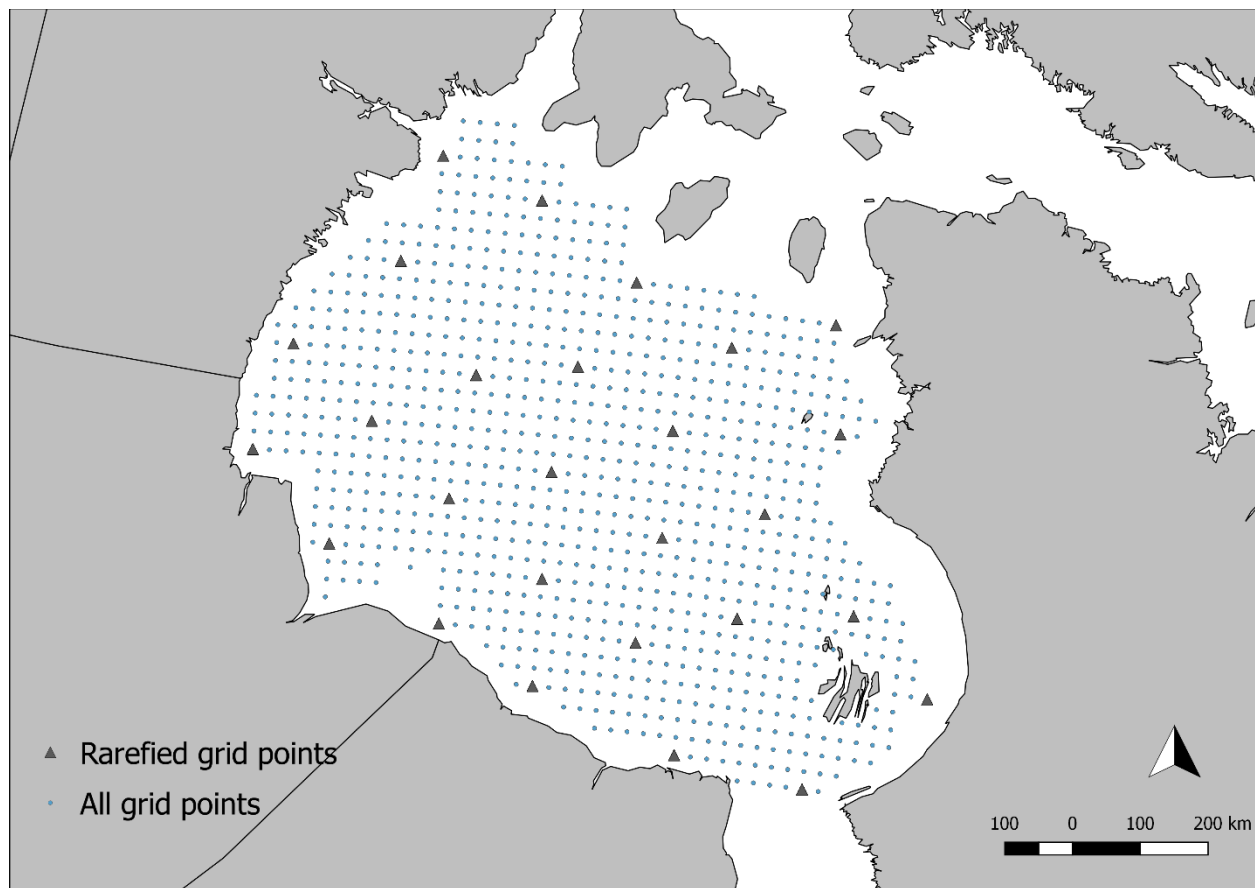


Fig S2. Original Polar Pathfinder ice motion vector grid points (“all grid points”) and the resulting rarefied data set obtained from the process explained above.

Table S1. Candidate models for assessing spatiotemporal trends in ice drift. All models included the same variables (ice speed ~ distance to coast + year + (1 | grid point ID)) and used a log-link function. Gamma models consistently had lower Akaike Information Criteria (AIC) scores (bolded).

Month	Model	AIC
November	Inverse Gaussian	20,616.00
	Gamma	<b>19,394.37</b>
December	Inverse Gaussian	102,319.10
	Gamma	<b>97,292.45</b>
January	Inverse Gaussian	116,421.85
	Gamma	<b>110,439.33</b>
February	Inverse Gaussian	103,700.00
	Gamma	<b>97,541.06</b>
March	Inverse Gaussian	113,877.60
	Gamma	<b>107,129.96</b>
April	Inverse Gaussian	108,603.26
	Gamma	<b>102,771.07</b>
May	Inverse Gaussian	107,276.10
	Gamma	<b>100,634.58</b>
June	Inverse Gaussian	78,821.91
	Gamma	<b>73,169.23</b>
July	Inverse Gaussian	22,212.23
	Gamma	<b>20,718.97</b>

Table S2. Candidate models for assessing the effect of ice drift on polar bear movement. All models included the same variables (bear movement ~ ice speed \* cosine + (1 | bearID)) and used a log-link function. Gamma models consistently had lower Akaike Information Criteria (AIC) scores (bolded).

Month	Model	AIC
November	Inverse Gaussian	-408.8
	Gamma	<b>-666.3</b>
December	Inverse Gaussian	-1419.2
	Gamma	<b>-1997.7</b>
January	Inverse Gaussian	-1624.5
	Gamma	<b>-2425.0</b>
February	Inverse Gaussian	-1941.1
	Gamma	<b>-2748.6</b>
March	Inverse Gaussian	-1820.1
	Gamma	<b>-2594.4</b>
April	Inverse Gaussian	-1512.1
	Gamma	<b>-2798.1</b>
May	Inverse Gaussian	-1754.8
	Gamma	<b>-2283.5</b>
June	Inverse Gaussian	-1126.4
	Gamma	<b>-1727.1</b>
July	Inverse Gaussian	-273.4
	Gamma	<b>-347.3</b>

*100% MCP results*

Generalized linear mixed effect models (GLMMs) assessing spatiotemporal trends in ice drift over the 100% MCP showed similar results to models assessing these same trends over the entire HB (Table S2). The 100% MCP GLMM assessing ice drift speeds over the year (November – July) also showed a negative trend ( $R^2 = 0.013$ ,  $p < 0.0001$ ). There was also a positive trend in CV over time ( $R^2 = 0.15$ ,  $df = 27$ ,  $p = 0.02$ ) (Figure S2).

Table S3. Mean ice drift (km/d) and coefficients of variation (CV) by month from 1987-2015 within the 100% MCP of adult female polar bears in western Hudson Bay, and results from generalized linear mixed effect models.  $R^2$  refers to the marginal  $R^2$  of the fixed effects, and  $R$  refers to the repeatability of the random effect (ice grid point ID). Bolded estimates represent a change in significance between the MCP model and the entire HB model (Table 1).

Month	Ice drift speed		Estimate			$R^2$	$R$
	Mean $\pm$ SD (km/d)	CV %	Intercept	Year	Distance to coast (km)		
November	5.0 $\pm$ 2.5	51.3	1.60	-0.02	0.02	0.005	0.008
December	4.8 $\pm$ 2.9	61.3	1.55	0.0002	0.08***	0.02	0.02
January	4.6 $\pm$ 3.2	68.5	1.52	<b>-0.006</b>	0.10***	0.02	0.03
February	4.2 $\pm$ 2.9	68.0	1.43	-0.03***	0.10***	0.02	0.03
March	4.2 $\pm$ 2.8	65.7	1.43	-0.06***	0.10***	0.03	0.03
April	4.2 $\pm$ 2.7	64.0	1.42	<b>-0.009</b>	0.09***	0.01	0.02
May	4.0 $\pm$ 2.3	56.6	1.39	-0.006	0.06***	0.01	0.01
June	3.6 $\pm$ 1.9	51.8	1.28	-0.01	0.06***	0.01	0.02
July	3.3 $\pm$ 1.9	56.3	1.18	-0.007	0.09***	0.02	0.03

\*\*\*  $p < 0.0001$

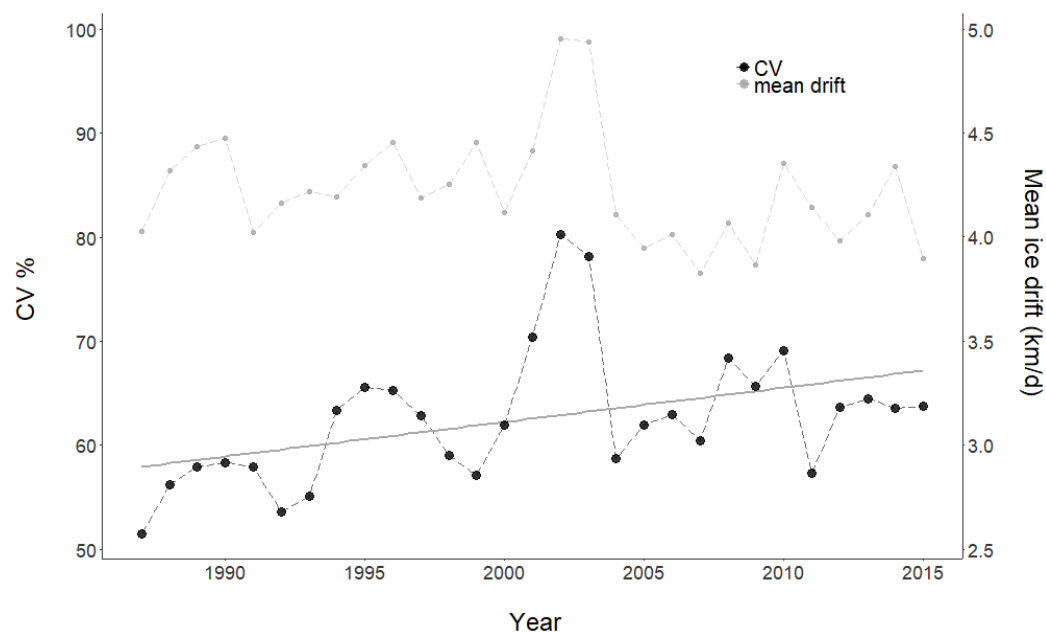


Fig. S3. Annual coefficients of variation (CV %) from 1987-2015 in the 100% MCP of adult female GPS-collared polar bears. Mean annual ice drift is included for reference (km/d). Ice drift estimates from Polar Pathfinder 25km EASE-Grid Sea Ice Motion Vectors. Line shows the significant trend of increasing CV across years ( $R^2 = 0.15$ ,  $df = 27$ ,  $p = 0.02$ ).

## References

Lavergne T, Eastwood S, Teffah Z, Schyberg H, Breivik LA (2010) Sea ice motion from low-resolution satellite sensors: An alternative method and its validation in the Arctic. *J Geophys Res Ocean* 115:C10032